

OIL SPILL DETECTION AND PREDICTION IN THE NW MEDITERRANEAN SEA: NEW MULTIFRACTAL METHODS FOR SAR ANALYSIS

Jose M. Redondo ⁽¹⁾ and Alexei Platonov ⁽¹⁾

(1) Dept. Física Aplicada, Univ. Politècnica de Catalunya, B5 Campus Nord UPC, Barcelona E-08034, (Spain)

ABSTRACT/RESUME

The oil pollution of Gulf of Lion in the NW Mediterranean has been studied with SAR images during the period 1999 -2005. We have analyzed these SAR images with respect to other surface features such as wind, river plumes, eddies and convergence areas. Some results of our statistical analysis are presented showing that the NW Mediterranean is most polluted along the main ship traffic routes, but comparatively less than near other routes in the Indian and the Pacific. The oil spill index is higher than one. The sizes of the detected oil spills vary over a large range, and if the statistics of the largest accidents are also considered on a longer timescale, we show that Zipf's Law, relating the frequency and the size of the spill in a hyperbolic fashion is applicable. Advanced image analysis techniques, such as the calculation of the multi-fractal dimensions of the observed SAR signatures, have been applied to distinguish between natural slicks and anthropogenic spills. Fractal dimensions can also be used to predict the time of release of the spill, non-dimensionalised with local turbulent dissipation. The multi-scale appearance and the topological structure of the slicks and spills may also be used as a useful measure of the diffusivity, yielding additional information which in turn may improve automated detection algorithms and be used in numerical models.

1 INTRODUCTION

The advances in satellite detection techniques in recent years have been able to highlight marine pollution and other previously ignored sea surface features such as vortices, fronts, convection areas, etc. There is also more public awareness to both the large nautical catastrophes (e.g. oil tankers Amoco Cadiz, Exxon Valdez and recently Erika and Prestige) and the habitual smaller oil spills from the ships. The range of marine pollution events should even consider, due to their overall importance, the very much smaller oil spills of a few square meters caused by small boats. The middle size oil spills often originate due to coastal sources and from small accidents or habitual cleaning of ballast water in ships. The larger oil spills are caused by crude/oil tankers catastrophic accidents of varied consequences but no systematic study except the CLEAN-SEAS project of the European Union [1,2] has been able to compare a wide range of detected oil spills. To obtain an updated vision of the dynamical processes and of the superficial pollution of the Northwest Mediterranean Sea we used results from SAR and ASAR and design strategies for oil spill detection and discrimination.

Extending and comparing statistically knowledge obtained during 1996-1998 with recent years (image data set, oil spills statistic temporal/spatial analysis, thematic maps) does not show significant changes. Improvements in software based in multi-fractal analysis applications allow to distinguish between the different detected sea surface phenomena, in particular it is important to be able to discriminate between natural slicks and oil spills as shown in figure 1.

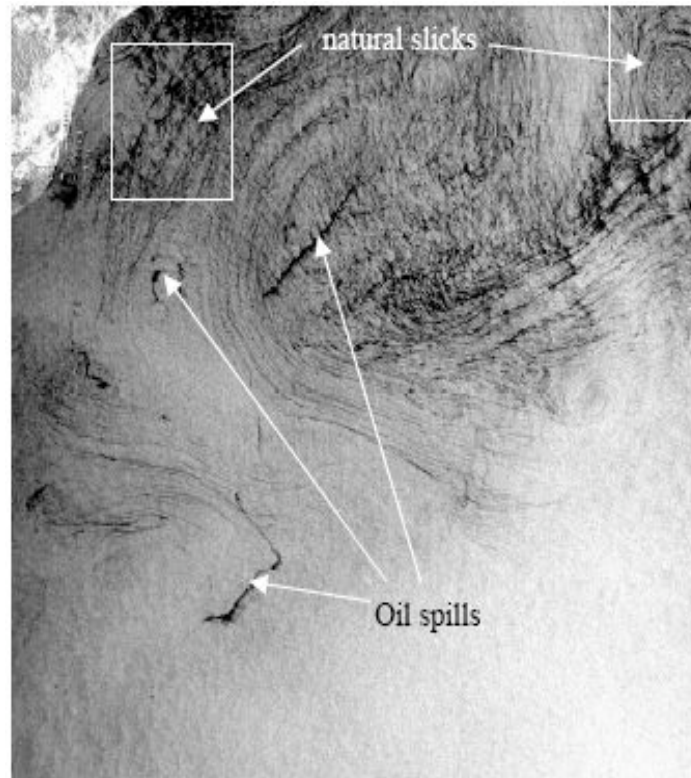


Fig. 1. Examples of oil spills and slicks in a SAR image near Barcelona.

2 OIL SPILLS, SLIKS AND SEA SURFACE FEATURES

The aim of this work is to apply our experience obtained during Clean Seas EU Project (1996-2000) and others, to extend and compare statistically our baseline knowledge of the state of the pollution in the North-western Mediterranean. The SAR images analysed, obtained during 1996-1998 were generally from the Clean Seas European project (near 900 images with 300 in the North-western Mediterranean Sea area). New images are obtained from ESA archives (ENVISAT and ERS-2 images during 1998-2003) as well as further SAR/ASAR images obtained directly from ESA contract (C1P.2240) (2000-2006). It is important to obtain a more updated vision of the associated sea surface dynamical processes in terms of the turbulent parameters needed to predict spill behaviour.

Also for other marine surface phenomena, such as vortices, fronts, convergence areas, etc, detected by SAR-ASAR the improvement in their statistic and the comparative analysis with in situ observations provides important data assimilation tools in order to improve numerical models of turbulent diffusion in the ocean surface at different scales.

In particular the role of the Rossby deformation radius on mesoscale turbulent diffusion will be discussed following references [3-6] considering the application of multifractal analysis to distinguish between antropogenic oil spills and natural slicks

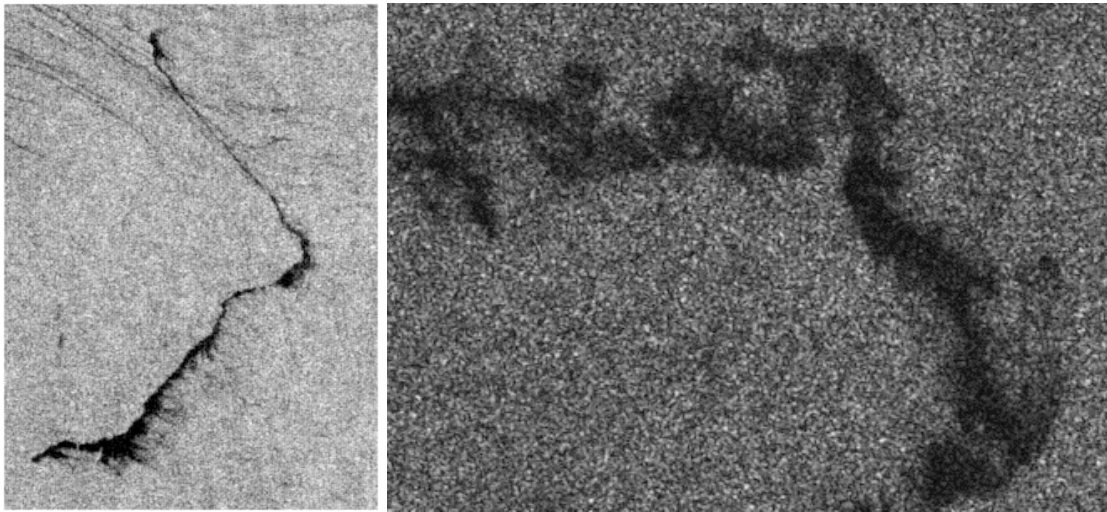


Fig. 2. Oil Spills of different sizes detected by ERS-2 (left) and ASAR ENVISAT (right) showing different weather histories and fractal dimensions.

Oceanic flow may be considered as turbulent motions under the constraints of geometry, stratification and rotation. At large scales these flows tend to occur mostly along isopycnal surfaces due to the combined effects of the very low aspect ratio of the flows (the motion is confined to thin layers of fluid) and the existence of stable density stratification. The effect of the Earth's rotation is to reduce the vertical shear in these almost planar flows. The combined effects of these constraints are to produce approximately a two-dimensional turbulent flow, there the nergy input at a given scale is transferred to larger scales, because these constraints stop vortex lines being stretched or twisted. Physically this upscale energy transfer occurs by merging of vortices and leads to the production of coherent structures in the flow that contain a significant part of the energy. This scenario is an appropriate model for geophysical flows which are known to contain very energetic meso-scale oceanic eddies. This upscale transfer of energy is inhibited at the Rossby deformation radius:

$$R_D = \frac{N}{f} h \quad (1)$$

where h is the characteristic scale of the depth of the thermocline and f the Coriolis parameter.

These dominant local vortices, together with the local turbulent cascade stretch and distort surface oil spills such as those of Fig. 2 at a wide of scales, see figure 3 for a compliation of the SAR detected eddies in the NW Mediterranean during 1996-1998. Most mixing processes in the ocean depend both on advection and diffusion characteristics with energetic inputs at many different scales, the topology of tracers in the ocean surface, probable depends on the local characteristics of the turbulent cascades.

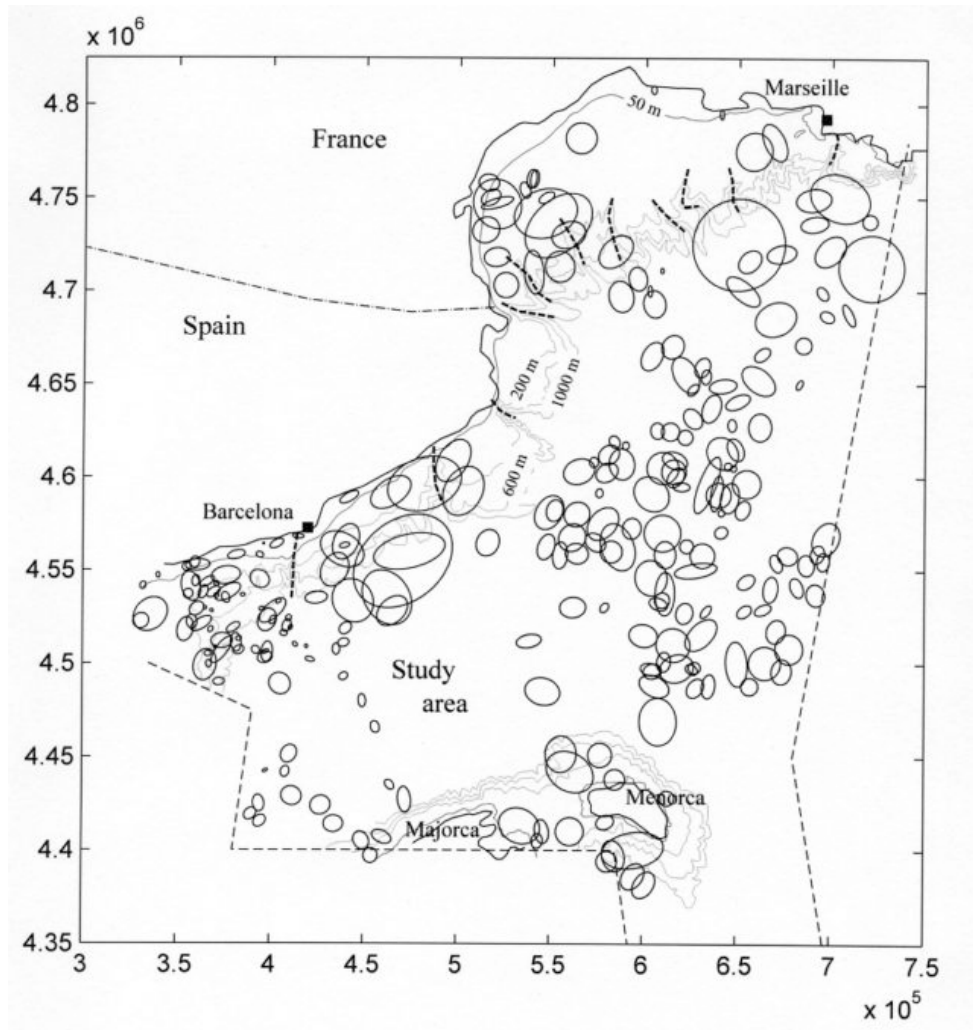


Fig. 3. Distribution of vortices detected by SAR in a 2 year period 1996-1998.

For example, in vortices in the ocean, local shear will transform slicks in the surface to align and follow the local flow so the resulting pattern is spiral. The mixing processes at large scale produce *stirring*, which maintains large gradients of the tracers. But in order to mix at molecular level in an irreversible fashion, the energy has to cascade to the smallest internal scales. In time the area where diffusion takes place increases and the variation of area in time may be used as a measure of the overall diffusion coefficient, K .

$$K = \frac{1}{2} \frac{d\sigma^2}{dt} \quad (2)$$

being σ a measure of the standard deviation of the size of the marked slick.

An important topological tool, fractal analysis was pioneered by Richardson and popularized by Mandelbrot. The fractal dimension is a very useful indicator of the complex environmental flow dynamics [4, 8], but it only reflects the self-similar geometry, not the dynamics of the flow. Because the oceans receive energy inputs at a wide range of scales this range where self-similarity takes place may describe the flow.

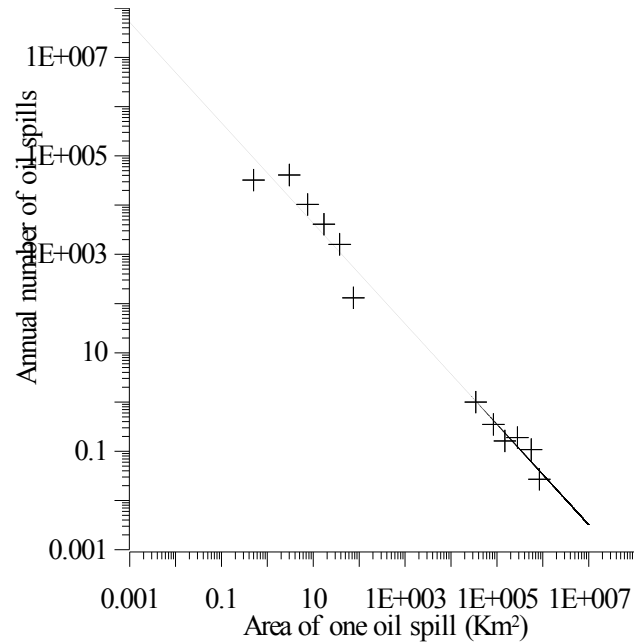


Fig. 4. Distribution of oil spills and large accidents in size, the Power fit in the log-log plot corresponds to Zipf's Law with slope -1 for European coastal waters.

3 ZIPF'S LAW; FRACTAL ANALYSIS ; OIL SPILL SIZE DISTRIBUTION

A comparative statistical analysis of both the last 40 years period tankers known shipwrecks in European coastal waters and the relatively small but common spills shows a power relation between the number of spills and their respective sizes over a seven decade interval. In the logarithmic scale this relation shows a good approximation to Zipf's law (law of increase of entropy) [7]. This basic law is simply described as $i f_i = C$, where i is the event rank, f_i is the frequency of its occurrence and C is a constant:

$$f_i \approx C i^{-a} \quad (2)$$

with f_i is the number of cases of the detection of the oil spills of a certain area rank and i is (the rank or complexity or size of the event (in our case, it is the average area of the spills)). Figure 4 shows such behaviour of oil spills in about seven decades in size.

Each set of values of an image property, which in the case of SAR detected oil is the level of reflectivity indicating surface roughness, has a certain fractal dimension, D , which expresses the level of self-similarity in space. This topological property may be studied. To calculate the fractal dimension, the Box-Counting method used produces a coverage of the object and the simplest method is to characterize it with boxes of side e . For the plane these boxes will be square and for an object in space they will be cubes. The distribution of the boxes is accomplished systematically, the intersection of these with the object carries the fact that we have N boxes with a non void intersection. For each one of these ranges it will be applied the usual fractal dimension calculation with the box-counting method and we will obtain the corresponding fractal dimension for each intensity level. The result of the process will be a set of dimension values,

function of the local SAR intensity relating the coverage of E sized boxes with their number as

$$D2 = - \frac{\ln N(E)}{\ln E} \quad (4)$$

By means of this methodology we have for each SAR intensity level, the corresponding value of the fractal dimension for different groupings of the levels allows a multi-fractal characterisation of the feature under study. [4,7,8]

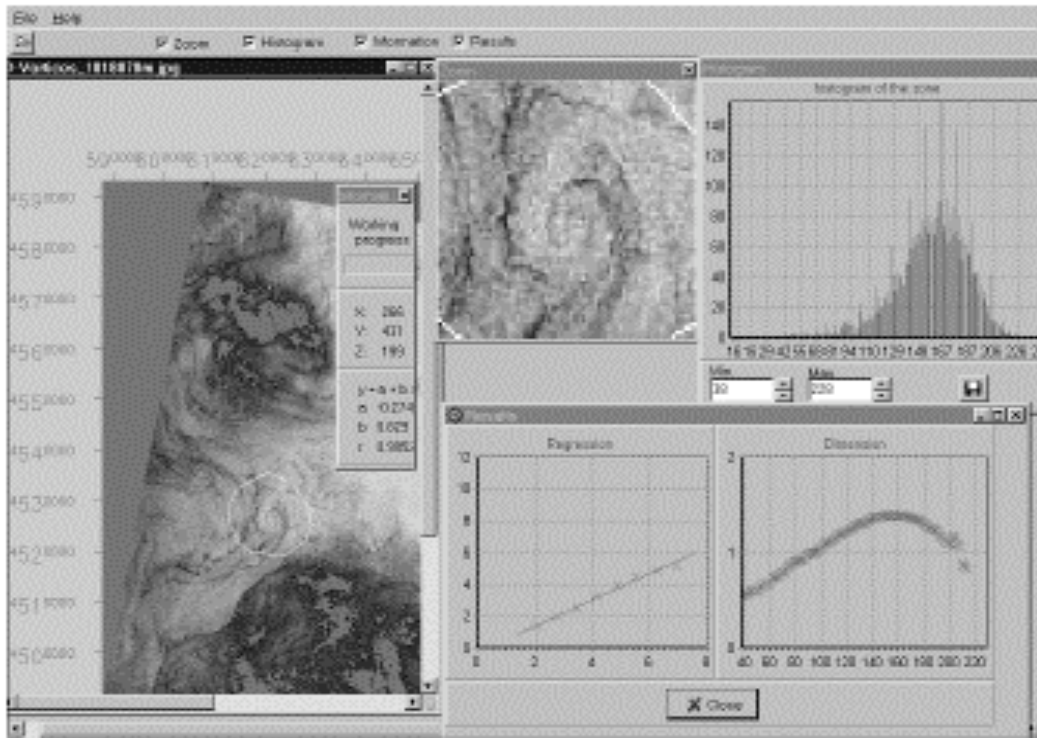


Fig.5. Example of the use of ImaCalc on a ERS-2 SAR image with both weather features and a recent oil spill (bottom) in the Northwest Mediterranean near Barcelona on 07.12.97. The image's box side size is about 100 Km.

An application of the multi-fractal analysis is the ability to discriminate between oil spills and natural slicks thanks to the time that a tracer takes to be in local equilibrium with the surrounding environmental velocity field.

The multi-fractal analysis of the different backscattered SAR intensity can be used to distinguish between natural and man-made sea surface features due to their distinct self-similar properties due to the time of residence in the ocean. Recent man-made oil spills in the sea surface are characterized by lower fractal dimension values ($D < 1.2$) over the region of low reflectivity in SAR images, on the other hand natural oil slicks show a typical parabolic shape with maximum of $D \gg 1.4$. Other local processes also affect the overall shape of the curves.

4 KINEMATIC SIMULATION OF OIL SPILL EVOLUTION

There are many ways to simulate a fluid flow, but when this is turbulent, these simulations become complicated, expensive and inaccurate. Using a Kinematic Simulation (KS) model, we have compared the evolution of spill shapes with different levels of local turbulence, with detected oil spills and field measurements.

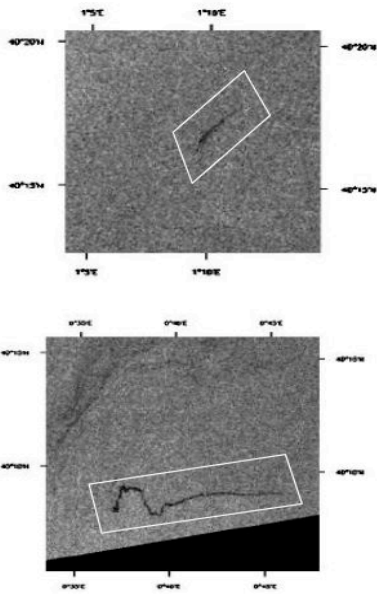


Figure 10. Two oil spills, which apparently have been detected during different times of evolution and diffused in the ocean surface. SAR images are shown at a resolution of about 1 pixel corresponding to 50 m.

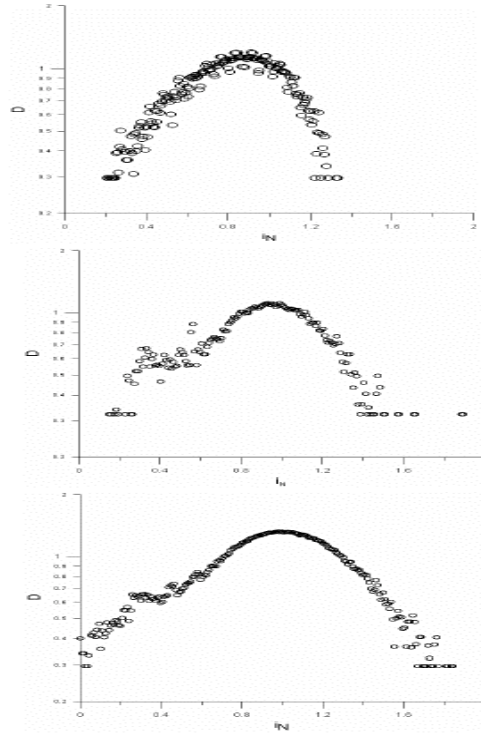


Figure 11. Multi-fractal analysis at a fixed grouping of 3 intensity levels of (above) a natural slick as shown in figure 7 and (below) the marked areas for the two oil spills of figure 9 during different times and diffused in the ocean surface (a logarithmic scale is used).

Fig.6. Multi-fractal analysis on different weathered oil spills from ERS-2 SAR images. Low fractal values for low reflective (dark) SAR intensities indicate recent oil spills.

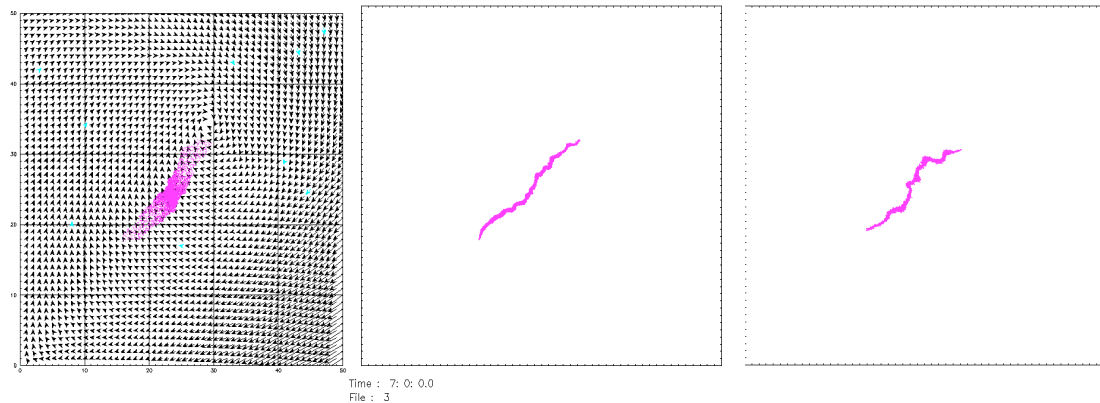


Fig. 7. Example of the turbulent dispersion of an oil spill with KSin velocity field (left)
Shape of two oil spills after the same time with different turbulence conditions.

To simulate the behaviour of oil spills (or tracer particles) in a turbulent flow, in a simple and efficient way that may be updated with the latest output from dedicated environmental wind and ocean currents with wave nested models. The dispersion of the spill is calculated with a Kinematic Simulation. This method has been reported to be useful for Lagrangian calculations. In KS, the velocity fluctuation is calculated as a Fourier series

$$\bar{u}'(\bar{x}, t) = \sum_{i=1}^N [\bar{a}_i \sin(\bar{k}_i \cdot \bar{x} + \omega_i t) + \bar{b}_i \cos(\bar{k}_i \cdot \bar{x} + \omega_i t)] \quad (5)$$

The vectors \bar{a}_i and \bar{b}_i give the energy of the mode i . So, they are related to the energy spectrum.

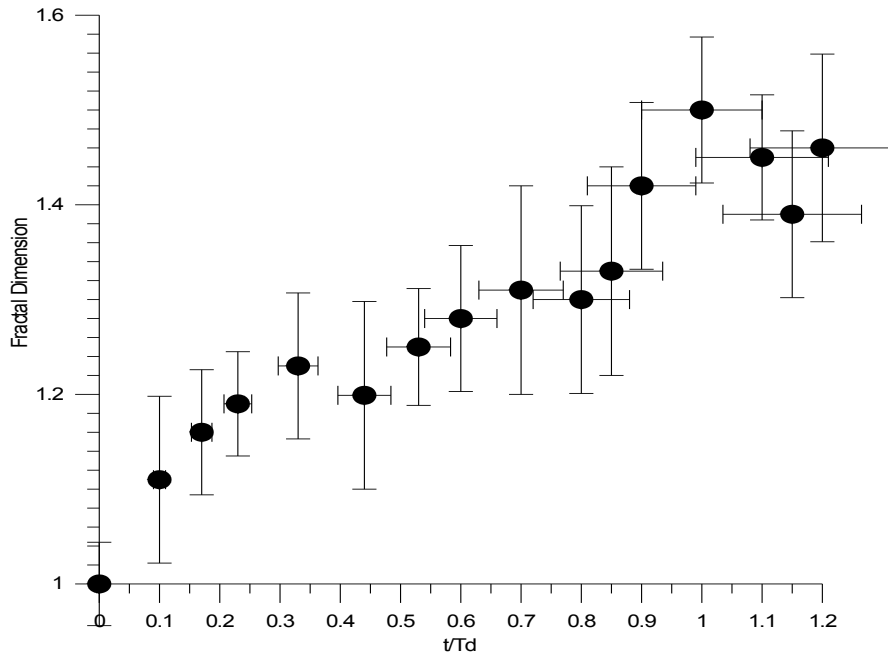


Fig. 8. Dependence of the maximum fractal dimension with non-dimensional time since the time of release of an oil spill using numerical simulations with KS model SpillSim.

These vectors are calculated through an integral balancing the energy at different wavenumbers k , such as:

$$\int_{k_i - 1/2\Delta k}^{k_i + 1/2\Delta k} E(k) dk \quad (6)$$

Where the energy spectrum (slope, limits and size) is given by the user. The program performs a second order Runge-Kutta with the motion equation

$$\frac{d\bar{X}_i(\bar{x}_0, t)}{dt} = v(\bar{X}(\bar{x}_0, t), t) \quad (7)$$

over 10000 neutrally advected particles. The velocity is the sum of the large scale field, calculated from the data given by the user, and the turbulence fluctuations that include a combination of all local effects (waves, wind, swell, coastal effects) calculated with the Kinematic Simulation as a turbulent intensity. For calculating the large scale velocity field, the user gives some vectors at some position in the domain. The program interpolates this data into a 100×100 grid. Such as those shown in figure 7. In figure 8 the evolution of the fractal dimension of the oil spill in time shows that scaling the time with a Damkholer number based on turbulent dissipation, T_D , the collapse is good.

5 DISCUSSION AND CONCLUSIONS

In principle it seems possible to find relationships that may be used to parameterise the sub-grid turbulence in terms of diffusivities that take into account the topology and the self-similarity of the sea surface environment. There is a need to calibrate the different regions determining the distribution of meso-scale vortices of size the Rossby deformation scale and other dominant features. Multi-fractal analysis can be used to distinguish fresh oil spills and natural slicks in the ocean surface, such as shown in Fig 9.

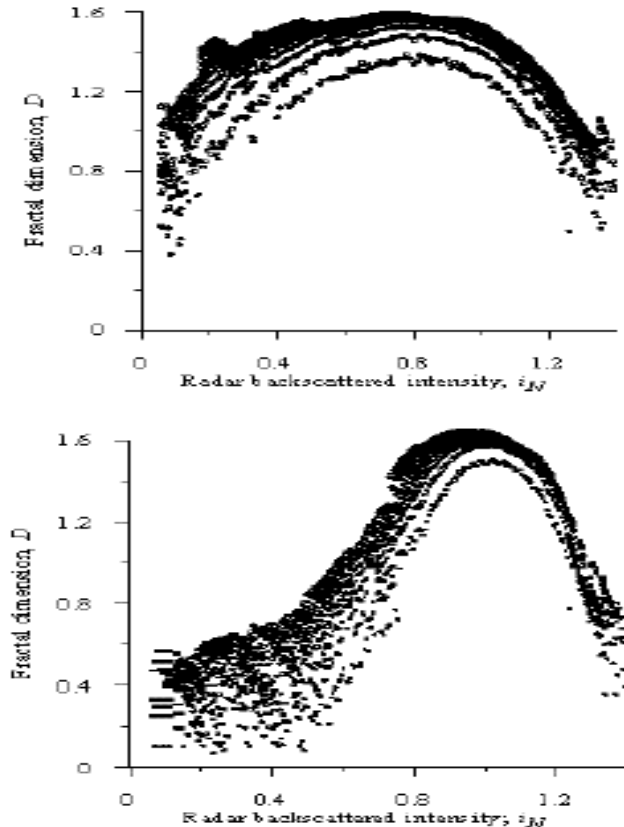


Figure 8 Multi-fractal analysis of the Natural slicks (above) and of the spill in the lower part of figure 7.

Fig. 9. Multifractal analysis of tensioactive natural slicks (above) and oil spill (below)

But with residence time the differences between them diminish. There is a Zipf's (power Law) scaling of detected oil spills up to large accidents. The European Coastal oil index is about 1-2, which is relatively small compared with the Malaca straits (4-6) [9], but other regions should be compared. The SAR images exhibited a large variation of natural features produced by winds, internal waves, the bathymetric distribution, by convection, rain, etc as all of these produce variations in the sea surface roughness so that the topological changes may be studied and classified [4-6,10-13].

7 REFERENCES

1. Jolly. G.W., A. Mangin, F. Cauneau, M. Calatuyud, V. Barale, H. M. Snaith, O.Rud, M. Ishii, M. Gade, J. M. Redondo, A. Platonov. The Clean Seas Project Final Report <http://www.satobsys.co.uk/CSeas/report.html>. ENV4-CT96-0334. Brussels. 2000.
2. Gade, M. and J M. Redondo. Marine pollution in European coastal waters monitored by the ERS-2 SAR: a comprehensive statistical analysis, IGARSS'99, Hamburg, Germany. pp. 1375-1377. 1999.
3. Carrillo, A., Sanchez, M.A., Platonov, A., Redondo, J.M. Coastal and Interfacial Mixing. Laboratory Experiments and Satellite Observations. Phy. Chem. of the Earth. Vol. B, 26/4. 2001.

4. Platonov A.K., J. Grau, J.M. Redondo. The structure and diffusion of the oil spills and slicks in the ocean Chashechkin and Baydulov (Eds.). RAS, Moscow. 2002.
5. Redondo, J. M. and Platonov, A. Aplicación de SAR en el estudio de la dinámica de las aguas y de la polución del mar Mediterráneo. Ingeniería del Agua, Vol. 8, 1, 2001.
6. Platonov, A.and Redondo, J. M. 2003 .Contaminación superficial del Mediterráneo Noroccidental Ingeniería del Agua. Vol 10, 2 , 149-162. 2003.
7. Zipf, G.K. Human Behaviour and the Principle of Least Effort. Hafner Publishing Company. New York, 1949

8. Mandelbrot, B.. The Fractal Geometry of Nature. Ed. W.H.Freeman and Company, New York. 1977.

9. Lu, J. Marine oil spill detection, statistics and mapping with ERS SAR imagery in south-east Asia. Int. J. Remote Sensing, No 15, 3013 – 3032. 2003.

10. Derbyshire, S.H. and Redondo, J.M. "Fractals and Waves, some Geometrical Approaches to Stably-Stratified Turbulence". *Anales de Física, Serie A*, Vol. 86, 1990.
11. Redondo, J.M. Mixing efficiency of different kinds of turbulent processes and instabilities. Applications to the environment. *Turbulent Mixing in Geophysical Flows*, Eds. Linden P.F. and Redondo J.M. CIMNE , Barcelona, 131-157. 2002.
12. Bezerra M.O., Diez M., Medeiros C., Rodriguez A., Bahia E. Sanchez-Arcilla A. y Redondo J.M. (1998) Study on the influence of waves on coastal diffusion using image analysis. *Jour. Flow Turbulence and Combustion*. 59, 191-204.
13. Redondo J.M. The topology of Stratified Rotating Flows in *Topics in Fluid Mechanics*, 129-135. Ed. Prihoda & K.Kozel, CAS, Praga 2004.